

A NEW APPROACH ACCOUNTING FOR SPECIES-SPECIFIC PLANT CHARACTERISTICS ON SAND CAPTURE EFFICIENCY IN AN AEOLIAN TRANSPORT MODEL

Quentin Laporte-Fauret, Oregon State University, quentin.laporte-fauret@oregonstate.edu
Meagan Wengrove, Oregon State University, meagan.wengrove@oregonstate.edu
Peter Ruggiero, Oregon State University, peter.ruggiero@oregonstate.edu
Sally D. Hacker, Oregon State University, sally.hacker@oregonstate.edu
Nicholas Cohn, US Army Engineer Research and Development Center, nicholas.t.cohn@usace.army.mil

INTRODUCTION

Coastal dunes are natural landforms that develop in the backshore of sandy coastlines through complex ecomorphodynamic interactions (Hesp, 2002). They provide a wide range of ecosystem services (Barbier et al., 2011) but are threatened by both increasing anthropogenic pressures and climate change (Vousdoukas et al., 2020). In most ecomorphodynamic numerical models which attempt to understand coastal dune evolution, the influence of vegetation on sediment transport is significantly simplified given the complexity of these interactions. Shear stress partitioning models are widely used to assess the effect of vegetation on wind force (Raupach, 1992; Okin, 2008), but to date only discriminate between vegetation type (e.g., grass, shrub, tree), without differentiating between the species-specific characteristics that play a role in the spatiotemporal evolution of dunes, their response to storms, and their recovery. Indeed, different dune grass species can build dunes of different shapes and sizes due to their unique ecological characteristics (Hacker et al., 2019). Using observations from a wind tunnel experiment that assessed sediment capture efficiency of the three main dune grass species of the U.S Pacific Northwest coast (the two non-native species *Ammophila arenaria*, AMAR, *Ammophila breviligulata*, AMAR, and the native species *Leymus mollis*, LEMO), the objective of this study is to develop model parameterizations that represent the sand capture efficiency of different dune grass species within a process-based aeolian sediment transport and dune evolution model.

MATERIALS AND METHODS

Zarnetske et al. (2012) conducted a wind tunnel experiment to investigate the sand capture efficiency of AMAR, AMBR and LEMO at three target densities (125, 250 and 500 tillers/m² planted in 1-m² boxes) and two wind speeds (6 m/s over 80 minutes per run and 9.5 m/s over 20 minutes per run). The proportion of the sand captured in the vegetated boxes (sand capture efficiency, C_e) was normalized to compare the results between the grass species and densities for a given wind speed, by dividing C_e by the non-dimensional volumetric sediment transport rate (q^*) (Zarnetske et al., 2012). For the statistical analysis and to conform to the assumption of linear regression, natural-log transformations were applied to $C_{e_{norm}}$. To numerically model the sand capture efficiency observed in the tunnel, the AeoliS process-based model was used (Hoonhout et al., 2016) in combination with the Bagnold equation for aeolian sediment transport (Bagnold, 1937) and the aerodynamic

roughness (z_0) equation developed by van Rijn et al. (2020). Vegetation was initially implemented in AeoliS via a value in each grid cell ranging from 0 (no vegetation) to 1 (fully vegetated). Vegetation height (m) was then approximated by the product of the maximum height of vegetation (m) and the root mean square of the vegetation cover fraction. The shear stress partitioning model developed by Okin (2008) was used to account for the effect of vegetation on sediment transport by:

$$\frac{u_{*,veg}}{u_*}(x) = R_0 + (1 - R_0) \left(1 + e^{-C_1 \frac{x}{h}}\right) \quad (1)$$

where u^* is the total friction velocity, $u_{*,veg}^*$ is the friction velocity component absorbed by the vegetation, $R_0 = u_{*,veg}/u_*$ for $x = 0$, x is the coordinate relative to the roughness element, C_1 is a factor controlling the shear stress recovery, and h is the height of the roughness elements (m). To consider the wind speed deceleration through the patch and the location where sand deposition begins, the canopy drag length (Belcher et al., 2003) and the deposition lag length (Dickey et al., 2023) were implemented in the AeoliS model. From wind tunnel videos of each run, the height of the canopy was measured and equations to calculate the leaf flexibility (F) as a function of the wind speed (u) and the tiller density (d_{veg}) were computed for each species (sp):

$$F_{sp} = a.u + b.d_{veg} + c \quad (2)$$

where a , b and c are coefficients. Leaf flexibility was used to compute an adjusted leaf height, allowing for computation of the frontal area of each tiller using the metrics of the species. The frontal area was computed as a product of the stem frontal area (height \times width) and the total leaf frontal area (adjusted height \times width \times number of leaves per tiller). The frontal area of each tiller was represented as a disk on a 1-mm resolution grid, with the stem at the center and a radius equal to the square root of the frontal area divided by π . All the cells in the disk were considered fully vegetated (i.e., value of 1). Upscaling algorithms were used to translate the 1-mm resolution vegetation grid to a resolution suitable for the model by computing the vegetation cover (from 0 to 1) in each upscaled (0.05 m) cell. In the simulations, we replicated the wind tunnel experiment of Zarnetske et al. (2012) with the same tunnel size, wind speeds, and tiller densities in the 1-m² box (with random tiller positions). In Okin's shear coupler, for each numerical experimental run, we set the C_1 coefficient to its default value, tested different R_0 values until we found the simulated $\ln(C_{e_{norm}})$ value closest to the observed data. A quadratic relationship between the vegetation density and the R_0 value for each species and wind speed was developed to extend the use

of the R_0 values in the sediment transport model to a wider range of grass densities. Finally, the accuracy of the simulated values of $\ln(C_{e_{norm}})$ compared to the observed values was estimated through R^2 , the Skill score (Skill, Willmott, 1981), and the Normalized Mean Bias (NMB).

RESULTS

For the three species, the simulated $\ln(C_{e_{norm}})$ values are similar to the wind tunnel observation data (Figure 1.a-c), with a high degree of agreement ($R^2 = 0.92$; Skill = 0.98 and NMB = -0.8%). The model accurately simulates the AMAR $\ln(C_{e_{norm}})$ values for all densities under both wind speeds ($R^2 = 0.95$; Skill = 0.99 and NMB = -0.11%) (Figure 1.a). Likewise, AMBR simulations have good agreement despite a slight underestimation of the simulated $\ln(C_{e_{norm}})$ at high densities under both wind speeds and a slight under- and over-estimation at low densities ($R^2 = 0.87$; Skill = 0.96 and NMB = +0.82%) (Figure 1.b). The simulated $\ln(C_{e_{norm}})$ values for LEMO mostly underestimated the observations for medium and high densities under both wind speeds but still show good agreement ($R^2 = 0.94$; Skill = 0.98 and NMB = -3.0%). Under low wind speed and for the lowest target density of each species in the experiment (i.e., 125 tiller/m²) we simulated sand deposition across a patch of vegetation (Figure 1d). LEMO, which had the greatest tiller frontal area given its wide and tall blades, had the shortest deposition lag length and the most sand deposition. AMBR, which had an intermediate tiller frontal area, showed a slightly longer lag in deposition and less overall sand deposition. Finally, AMAR, which has the smallest frontal area due to its thinner and shorter leaves, has the longest deposition lag length and the least sand deposition.

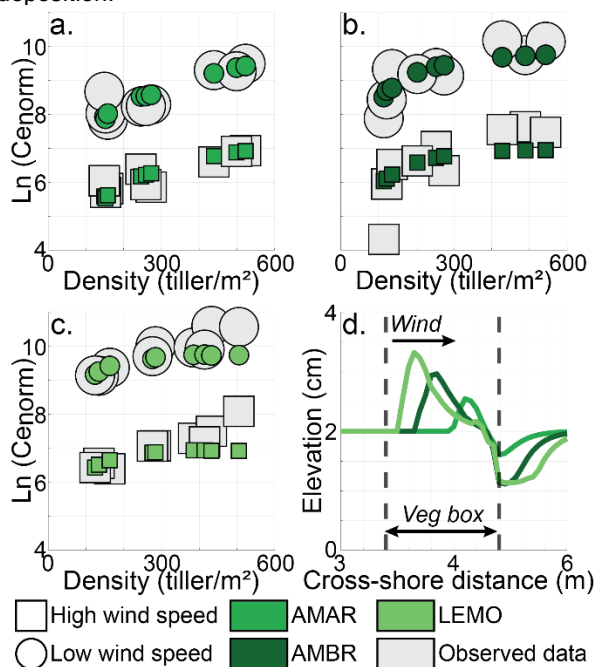


Figure 1 - Sand capture efficiency, $\ln(C_{e_{norm}})$ for (a) AMAR, (b) AMBR and (c) LEMO. Observed data are in grey and simulated data with R_0 computed by the quadratic relation are in shade of green. (d) Average cross-shore profiles in the vegetated box for the three species at the end of the

simulations with 125 tiller/m² under 6.5 m/s wind speed.

CONCLUSIONS

In this study, we developed a new approach to simulate the sand capture efficiency of three dune grass species and model sand deposition in a process-based aeolian sediment transport and dune morphologic change model. The model was tested against wind tunnel observations of sediment capture within stands of vegetation and showed excellent agreement for all three dune grass species and wind speeds. We also modelled sand deposition patterns similar to those in the wind tunnel experiment (LEMO > AMBR > AMAR) but note that under field conditions, AMAR and AMBR remain the best at sand accretion and dune building due to their greater tiller densities and growth form traits in nature (Zarnetske et al. 2012). While more calibration remains, this study offers a first step in incorporating species-specific effects into models designed to replicate the shape and size of coastal foredunes.

REFERENCES

- Bagnold (1937): The transport of sand by wind, *The Geographical Journal*, 89(5), 409.
- Barbier, Hacker, Kennedy, Koch, Silliman, Stier (2011): The value of estuarine and coastal ecosystem services, *Ecological Monographs*, 81, 169-193.
- Belcher, Jerram, Hunt (2003): Adjustment of a turbulent boundary layer to a canopy of roughness elements, *Journal of Fluid Mechanics*, 488, 369-398.
- Dickey, Wengrove, Cohn, Ruggiero, Hacker (2023): Observations and modeling of shear stress reduction and sediment flux within sparse dune grass canopies on managed coastal dunes, *Earth Surface Processes and Landforms*, 48(5), 907-922.
- Hacker, Jay, Goldstein, Hovenga, Itzkin, Moore, Mostow, Mullins, Reeves, Ruggiero (2019): Species-specific functional morphology of four US Atlantic coast dune grasses: biogeographic implications for dune shape and coastal protection, *Diversity*, 11, 82.
- Hesp (2002): Foredunes and blowouts: initiation, geomorphology and dynamics, *Geomorphology*, 48, 245-268.
- Hoonhout, de Vries (2016): A process-based model for aeolian sediment transport and spatiotemporal varying sediment availability, *Journal of Geophysical Research: Earth Surface*, 121(8), 1555-1575.
- Okin (2008): A new model of wind erosion in the presence of vegetation, *J of Geophysical Research*, 113, F02S10.
- Raupach (1992): Drag and drag partition on rough surfaces, *Boundary-Layer Meteorology*, 60(4), 375-395.
- Van Rijn, Strypsteen (2020): A fully predictive model for aeolian sand transport, *Coast Eng*, 156, 103600.
- Vousdoukas, Ranasinghe, Mentaschi, Plomaritis, Athanasiou, Luijendijk, Feyen (2020): Sandy coastlines under threat of erosion, *Nat. Clim. Chang.* 10 (3), 260-263.
- Willmott (1981): On the validation of models, *Physical Geography*, 2, 184-194.
- Zarnetske, Hacker, Seabloom, Ruggiero, Killian, Maddux, Cox (2012): Biophysical feedback mediates effects of invasive grasses on coastal dune shape, *Ecology*, 93, 1439-1450.